



This is a repository copy of *Planar organic spin valves using nanostructured Ni₈₀Fe₂₀ magnetic contacts*.

White Rose Research Online URL for this paper:
<http://eprints.whiterose.ac.uk/96457/>

Version: Accepted Version

Article:

AlQahtani, H., Bryan, M.T., Hayward, T.J. et al. (5 more authors) (2014) Planar organic spin valves using nanostructured Ni₈₀Fe₂₀ magnetic contacts. *Organic Electronics*, 15 (1). pp. 276-280. ISSN 1566-1199

<https://doi.org/10.1016/j.orgel.2013.11.009>

Article available under the terms of the CC-BY-NC-ND licence
(<https://creativecommons.org/licenses/by-nc-nd/4.0/>)

Reuse

This article is distributed under the terms of the Creative Commons Attribution-NonCommercial-NoDerivs (CC BY-NC-ND) licence. This licence only allows you to download this work and share it with others as long as you credit the authors, but you can't change the article in any way or use it commercially. More information and the full terms of the licence here: <https://creativecommons.org/licenses/>

Takedown

If you consider content in White Rose Research Online to be in breach of UK law, please notify us by emailing eprints@whiterose.ac.uk including the URL of the record and the reason for the withdrawal request.



eprints@whiterose.ac.uk
<https://eprints.whiterose.ac.uk/>

Planar organic spin valves using nanostructured Ni₈₀Fe₂₀ magnetic contacts

Hadi AlQahtani^{1,4,*}, Matthew T Bryan², Thomas J Hayward², Matthew P Hodges², M-Y Im³, Peter Fischer³, Martin Grell¹, Dan A Allwood²

¹Department of Physics and Astronomy, University of Sheffield, Sheffield, S3 7RH, UK,

²Department of Materials Science and Engineering, University of Sheffield, Sheffield, S1 3JD, UK

³Center for X-ray Optics, Lawrence Berkeley National Laboratory, Berkeley, CA, USA

⁴Department of Physics and Astronomy, College of Science, King Saud University, Riyadh, Saudi Arabia.

*Corresponding author, hralqahtani@ksu.edu.sa

Abstract

Planar organic spin valves were fabricated by evaporating organic semiconductor PTCDI-C₁₃ onto pairs of patterned Ni₈₀Fe₂₀ magnetic nanowires separated by 120 nm. Control over the relative alignment of magnetisation in the nanowires was achieved by including a domain wall 'nucleation pad' at the end of one of the wires to ensure a large separation in magnetic switching fields. Switching behavior was investigated by optical and x-ray magnetic imaging. Room temperature organic magnetoresistance of -0.35% was observed, which is large compared to that achieved in vertical spin valves with similar materials. We attribute the enhanced performance of the planar geometry to the deposition of the semiconductor on top of the metal, which improves the quality of metal-semiconductor interfaces compared to the metal-on-semiconductor interfaces in vertical spin valves.

Introduction

Organic semiconductors (OSCs) have attracted interest as potential charge/spin transport materials for use in spintronic devices, in which electron spin as well as charge is used to perform operations. Despite their low charge carrier mobilities, OSCs are in demand due to their low spin-orbit coupling and weak hyperfine interactions, which help to maintain spin polarisation for longer distances than is achievable in inorganic materials [1]. The scope and rationale for introducing spin transport phenomena into OSC devices (and *vice versa*) was reviewed by Dediu *et al.* [2].

The most significant component in spintronic technology to date is the spin valve. This consists of two ferromagnetic (FM) contacts connected by a non-magnetic layer, which couples magnetic behaviour to electrical transport. When current flows through the device, one FM contact acts to polarise and the other to analyse the spin of the charge carriers, such that the resistance of the device depends on the relative orientation of the FM contact magnetisations. The magnetoresistance, MR, of the device is defined as

$$\text{MR} (\%) = \frac{R_{PP} - R_{AP}}{R_{AP}} \times 100\% \quad (\text{eq. 1})$$

where R_P and R_{AP} are the resistance values of the device when the FM contact magnetisations are parallel (P) and anti-parallel (AP), respectively. The magnitude of the MR depends on the spin polarisation in the FM contacts, the physical mechanism responsible for the resistance (tunnelling or scattering at layer interfaces) and the material used in the non-magnetic layer [3]. When the non-magnetic layer is an organic semiconductor, *negative* MR is commonly observed ($R_{AP} < R_P$) [4-8]. A possible explanation has been proposed by Schulz *et al.* [7], based on the assumption that injected carriers do not reflect the bulk (average) spin polarisation of the contact, but the spin polarisation at the energy level corresponding to the relevant OSC transport level (highest occupied molecular orbital [HOMO] for hole transport; lowest unoccupied molecular orbital [LUMO] for electron transport), which may be negative compared to bulk polarisation.

In principle, the use of an OSC as the non-magnetic layer in the spin valve should enhance the MR, due to their minimal interaction with charge carrier spin. Indeed, organic spin valves (OSVs) at cryogenic temperatures have been observed with MR values between -40% and -300% [8,9,10]. However, at room temperature, the MR commonly drops to around -0.1% [4-7]. Such low room temperature MR values could be due to the vertical geometry (layers stacked on top of each other) employed to achieve sub-100 nm contact spacing, since the topmost interface suffers damage during the deposition of the FM contact onto the inherently soft OSC layer. Sun *et al.* demonstrated the importance of the organic/FM interface quality by showing that OSVs protected by a frozen xenon buffer

layer during deposition of the top FM contact exhibited a 17-fold increase in MR compared to unprotected OSVs [9].

Here, we describe the fabrication of planar FM contact electrodes for OSVs to avoid the 'top-interface' problem altogether and obtain larger MR magnitudes than similar vertical systems. The FM contacts are co-planar but separated by a narrow gap, with the organic semiconductor deposited on top. The deposition of the organic semiconductor on to the FM metal causes little interfacial damage, so the planar geometry is intrinsically more robust than vertical OSVs. However, there are several challenges to fabricating planar OSV structures, which may have inhibited previous investigations of planar OSVs. By using a single magnetically soft material for both FM electrodes, we simplify the fabrication process and enable the shape of the electrodes to be used to separate their coercivities, providing access to both the P and AP configurations. A similar planar spin-valve has previously been demonstrated using graphene [11] but the MR was extremely small. The planar OSV reported by Kawasugi *et al.* [12] had a much longer gap between FM contacts, deposited both contacts on top of the organic (rather organic on top of both contacts), and showed no measurable MR.

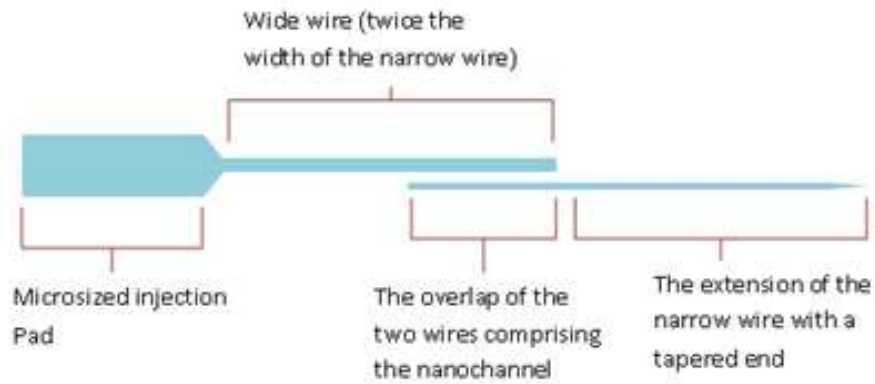
Experimental

Planar OSVs were fabricated in three stages. First, five pairs of magnetic contact nanowires (Fig. 1) were patterned by electron beam lithography into a poly(methylmethacrylate) (PMMA) resist, thermal evaporation of Permalloy (Ni₈₀Fe₂₀) and subsequent lift-off of the remaining resist. Lithography was performed at an electron beam energy of 10 keV, designing the nanowire spacing to compensate for the narrowing of the channel between them due to the dose proximity effect (additional removal of resist caused by the overlap of neighboring electron beam dose profiles). Second, non-magnetic Ti(20 nm)/Au(200 nm) electrodes were fabricated on top of the nanowires using photolithography, contacting the five pairs of nanowires in parallel, to enable electrical connectivity using spring clips. The non-magnetic electrodes were separated by 150 μm to ensure that current flowed through the magnetic nanowires. These structures were comprehensively characterised for their magnetic behaviour first, before completing the planar OSVs by evaporating a 50 nm thick film of the low molecular weight, electron-transporting OSC N,N'-ditridecyl perylene diimide with α,ω - C₁₃H₂₇ alkyl chains (PTCDI-C₁₃; Fig. 1d). We preferred PTCDI-C₁₃ over Alq₃, which was often used in OSV research previously [7-10]. The prevalence of Alq₃ is probably for historic [13] rather than scientific reasons: PTCDI-C₁₃ has higher charge carrier mobility, a deeper LUMO for better electron injection [14, 15] and avoids a metal core that may act as spin scattering centre.

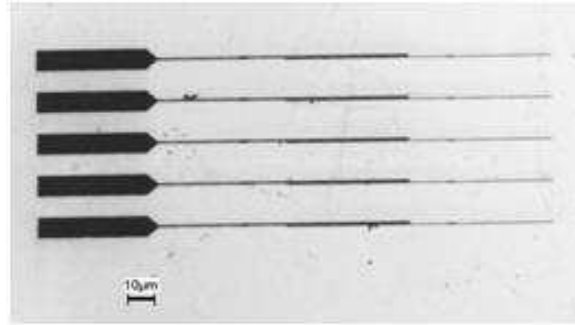
Two sets of samples were prepared: one onto intrinsically doped (high resistivity) Si (001) with a native oxide for electrical characterisation and examination using magneto-optical

Kerr effect (MOKE) magnetometry with a focussed laser spot of $\sim 5 \mu\text{m}$ diameter [16]; and another (without the photolithography or organic deposition stages) onto 100 nm thick Si_3N_4 membranes for magnetic transmission X-ray microscopy (M-TXM) [17]. M-TXM was performed at beamline 6.1.2 at the Advanced Light Source in Berkeley, CA, using circularly polarised soft x-rays tuned to the Fe L_3 (706 eV) X-ray absorption edge. M-TXM is capable of imaging magnetic domain walls [18], achieving in-plane magnetic contrast through X-ray magnetic circular dichroism (X-MCD) by tilting the sample by 60° with respect to the photon propagation direction. Magnetic contrast is obtained relative to a reference image, taken under a saturating magnetic field of $B = -100 \text{ mT}$. This causes any change in configuration from saturation to be observed as dark contrast.

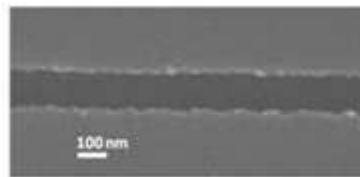
The wires in each set were 1000 nm and 500 nm wide, separated by a gap (channel length, L) of 120 nm. Together with the addition of a nucleation pad attached to the wider wire, the different wire widths ensured that the wires had different coercive fields [19-21], enabling the device to operate as an in-plane OSV. In the Si substrate sample, the Permalloy nanowires were 30 nm thick, the lateral overlap of the nanowire pairs (channel width, W) was $60 \mu\text{m}$, and the nucleation pad was $10 \mu\text{m}$ wide and $59 \mu\text{m}$ long. To optimize the magnetic contrast in the M-TXM images, the sample on the Si_3N_4 substrate was fabricated with Permalloy thickness 40 nm, $W = 5 \mu\text{m}$ and a $6 \mu\text{m}$ wide, $39 \mu\text{m}$ long nucleation pad.



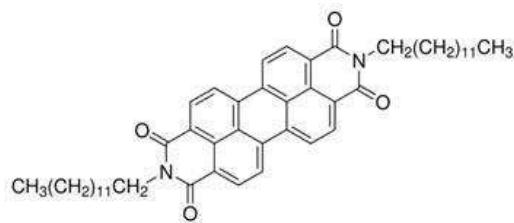
(a)



(b)



(c)



(d)

Figure 1. (a) Schematic design of contact wire pair. Note the different width of the nanowires, and the tapered end of the thinner wire. (b) Electron micrograph of a group of five contact wire pairs. (c) A higher resolution image of the channel region of one contact wire pair (Magnetic wires appear light and the channel dark). (d) Structure of the PTCDI-C₁₃ organic semiconductor used here.

Magnetic characterisation

For the FM contacts to be useful for OSVs, the following two requirements have to be met: firstly, each electrode's magnetisation has to lie along the wire length (orthogonal to the direction of charge transport), so that the relative magnetic configuration of the wires will be either 'parallel' (P), or 'anti-parallel' (AP); secondly, the two wires need to have different coercive fields, so that the P and AP configurations are accessible with the external application of magnetic fields. Here, the first requirement is met by the intrinsic shape anisotropy and near-zero magnetocrystalline anisotropy of the Ni₈₀Fe₂₀ nanowires [22]. The second requirement can be satisfied by using the nanowire shape to control the nucleation and propagation of domain walls. Although wider nanowires tend to have lower

coercivities [19], the reversal behaviour is dominated by our use of the large pad to support domain wall nucleation at low applied fields [23] and tapering the ends of the other wire to suppress reverse domain nucleation [24]. Before proceeding to OSV manufacture and electric characterisation, we carried out a detailed magnetic characterisation of the contact electrodes to confirm the above requirements were met and that there is no stray field interaction between the adjacent wires.

Figure 2a shows the normalised magnetisation response (M/M_s) using MOKE magnetometry of individual wires and the region where the wires overlap, for the field direction parallel to the wire long axis. The wider wire switched at 3.6 mT and the narrower wire at 14.9 mT, establishing a large field region over which the AP configuration of the device can be selected. There is little change in the switching field in the overlap region, indicating that the nanowires switch independently within the region of the OSV channel, by injection and propagation of a magnetic domain wall.

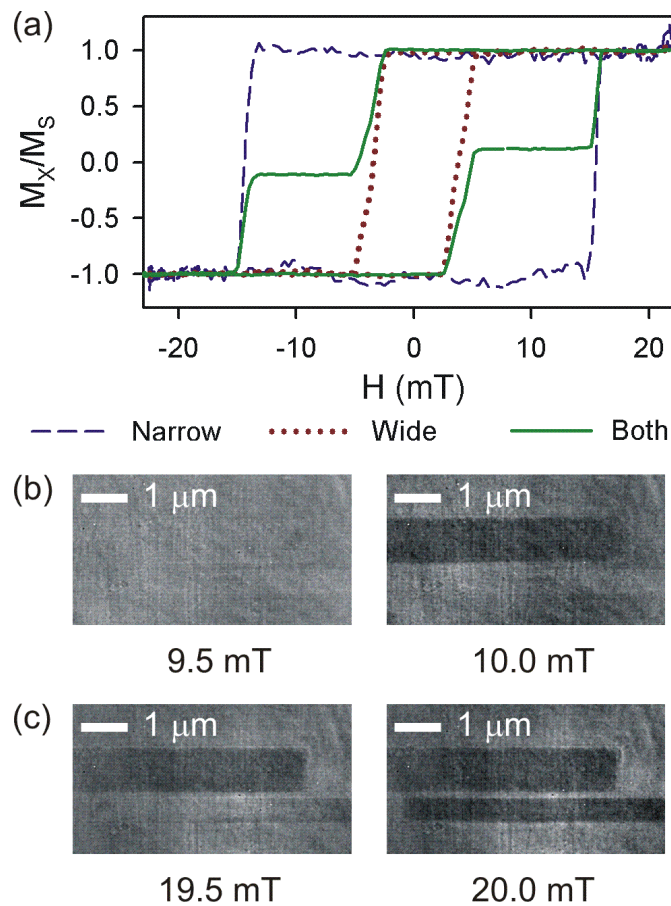


Figure 2. (a) Normalised magnetisation (M/M_s) hysteresis loop obtained using MOKE magnetometry, taken after positioning the laser spot over the narrow (500 nm) wire, wide

(1 μm) wire and over both wires in the overlap region forming the OSV channel. **(b)** and **(c)** M-TXM images showing switching in **(b)** the wide wire at 10 mT and in **(c)** the narrow wire at 20 mT. The images are normalised relative to saturation at -100 mT, such that magnetisation reversal appears as dark contrast, while magnetisation that is unchanged from saturation has the same contrast as the background.

To confirm that switching occurred without any interaction between the wires, we imaged the magnetisation directly using M-TXM (fig. 2b and c). The switching fields of the imaged wires differed from those probed using MOKE due to the different sample thickness and pad size used. Nevertheless, the M-TXM images confirm that the structure switches from the P to the AP configuration via the reversal of the wide wire (fig. 2b) and then, at higher fields, switches back from the AP state to the P configuration via the reversal of the narrow wire (fig. 2c). Furthermore, the abrupt switching shown in the images demonstrates that the domain walls mediating the reversal of the magnetisation in each wire are not pinned by the stray field from the adjacent wire end. This is in contrast to previous observations of domain wall pinning caused by adjacent elements arranged perpendicular to the nanowire [25] or domain walls in nearby nanowires [26,27].

Electrical characterisation

After magnetic characterisation of our magnetic contacts, we evaporated PTCDI-C₁₃ to create the OSVs. Initial electric characterisation of resulting planar FM(1) : OSC : FM(2) spin valves was carried out in the absence of any magnetic fields, using a Keithley source-measure unit.

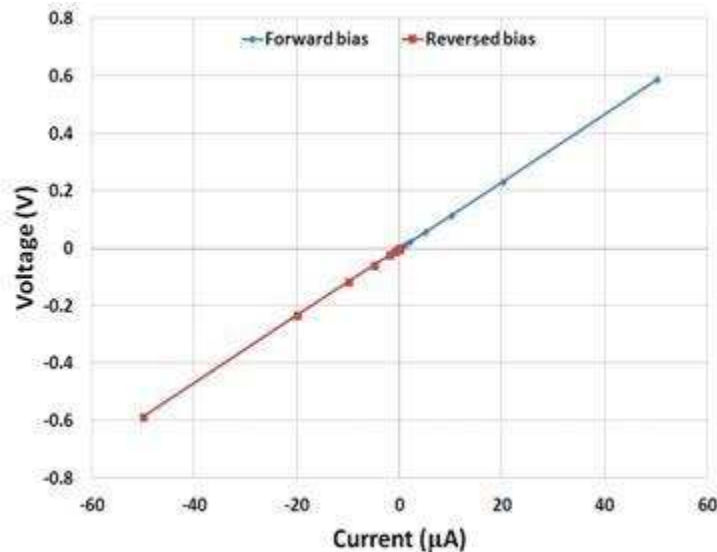


Figure 3. I-V characteristic of wide Ni₈₀Fe₂₀ / PTCDI-C₁₃ / narrow Ni₈₀Fe₂₀ planar OSV in the absence of external magnetic field.

The OSV shows ohmic I-V characteristics, without curvature, hysteresis, or asymmetry (Fig. 3). This shows that there is reasonably efficient carrier injection at the $\text{Ni}_{80}\text{Fe}_{20}$ / PTCDI- C_{13} junction, although this does not rule out a degree of spin scattering at injection. The resistance of the planar OSV was $12\text{ k}\Omega$, significantly lower than e.g. the device of Sun *et al.* [9].

Magnetoresistance (MR) was measured under constant-current conditions (500 nA) at ambient temperature and pressure by monitoring the voltage drop over the OSV while sweeping magnetic field induction from -25 mT to $+25\text{ mT}$ at 0.2 mT/sec and averaging data over ten field cycles. The observed MR loop (Fig. 4) has two distinct transitions in each field sweep direction, which correspond well to the P and AP magnetic configurations described earlier. The MR transitions are not as sharp as those measured by MOKE from individual wires (Fig. 2a). This is probably due to variations in the switching fields between wires in the five devices we characterise in parallel for MR. Quantitatively, we find MR of -0.35% .

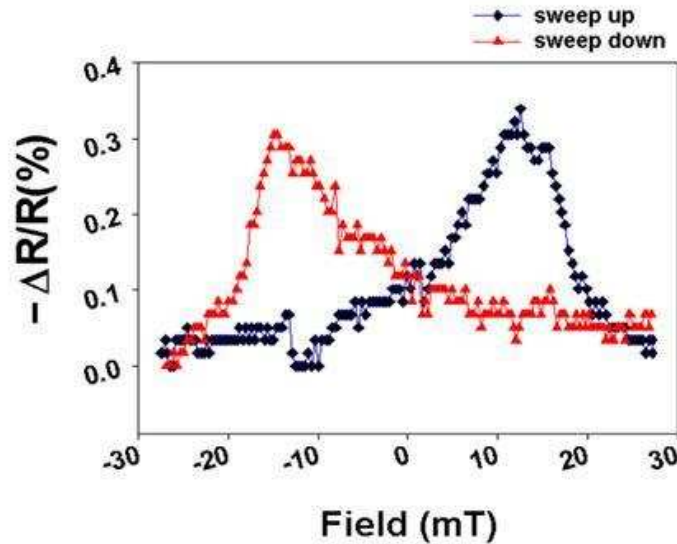


Figure 4. Magnetoresistance loop of $\text{Ni}_{80}\text{Fe}_{20}$ /PTCDI- C_{13} planar OSV.

MR with negative sign is commonly observed for OSVs at ambient temperature [4-9]; we refer to the possible explanation given by Schulz *et al.* [7]. The modulus of ambient temperature MR observed here for a planar OSV is similar or higher than in typical vertical OSVs. For comparison, about -0.15% magnetoresistance was obtained at RT with a vertical SV of LSMO/ Al_2O_3 /Alq₃/Co [28] while -0.1% was achieved with Co / Fe alloy magnetic contacts using a vertical geometry of $\text{Co}_{50}\text{Fe}_{50}$ /P3HT/ $\text{Ni}_{80}\text{Fe}_{20}$ [6].

Conclusions

We have demonstrated a planar organic spin valve architecture that avoids the problems of metal-on-organic interfaces. This configuration is, therefore, well suited for investigating spin-polarised electron transport in organic semiconductors with much less uncertainty about interface quality and separation than is the case with vertical spin valve arrangements. Pairs of coplanar Ni₈₀Fe₂₀ contact nanowires with narrow separations and differences in geometry allowed parallel and anti-parallel magnetic configurations in the contacts to be selected easily with an externally applied magnetic field. Spin valves fabricated by the subsequent evaporation of the electron-transporting organic semiconductor PTCDI-C₁₃ allowed observation of -0.35% magnetoresistance at room temperature. The negative sign is commonly observed for organic MR and can be explained by the difference between extracted and bulk (or Fermi level) spin polarisation of the magnetic electrodes. The modulus of MR is comparatively large for room temperature organic MR, suggesting higher quality interfaces than is achieved in vertical spin valves.

Acknowledgements

HA would like to thank King Saud University for the sponsorship of his PhD studies. MPH thanks EPSRC for a DTA studentship. TJH acknowledges the support of EPSRC through EP/J002275/1. The operation of the x-ray microscope work was supported by the Director, Office of Science, Office of Basic Energy Sciences, Materials Sciences and Engineering Division, of the U.S. Department of Energy under Contract No. DE-AC02-05-CH11231.

References

1. Naber, W.J.M., S. Faez, and W.G. van der Wiel, Organic spintronics. **Journal of Physics D-Applied Physics**, 2007. 40(12): p. R205-R228.
2. Dediu, V.A., et al., Spin routes in organic semiconductors. **Nature Materials**, 2009. 8(9): p. 707-716.
3. Julliere, M., Tunneling between Ferromagnetic-Films. **Physics Letters A**, 1975. 54(3): p. 225-226.
4. Majumdar, S., et al., Application of regioregular polythiophene in spintronic devices: Effect of interface. **Applied Physics Letters**, 2006. 89(12).
5. Dediu, V., et al., Room-temperature spintronic effects in Alq₃-based hybrid devices. **Physical Review B**, 2008. 78(11).
6. Morley, N.A., et al., Room temperature organic spintronics. **Journal of Applied Physics**, 2008. 103(7).
7. Schulz, L., et al., Engineering spin propagation across a hybrid organic/inorganic interface using a polar layer. **Nature Materials**, 2011. 10(1): p. 39-44.
8. Xiong, Z.H., et al., Giant magnetoresistance in organic spin-valves. *Nature*, 2004. 427(6977): p. 821-824.
9. Sun, D.L., et al., Giant Magnetoresistance in Organic Spin Valves. **Physical Review Letters**,

2010. **104**(23).

10. **Barraud, C., et al.**, Unravelling the role of the interface for spin injection into organic semiconductors. **Nature Physics**, 2010. **6**(8): p. 615-620.

11. **Ohishi, M., et al.**, Spin injection into a graphene thin film at room temperature. **Japanese Journal of Applied Physics Part 2-Letters & Express Letters**, 2007. **46**(25-28): p. L605-L607.

12 Y Kawasugi, M Ara, H Ushirokita, T Kamiya, H Tada, Preparation of lateral spin-valve structure using doped conducting polymer poly(3,4-ethylenedioxythiophene) poly(styrenesulfonate), **Organic Electronics**, 2013, **14**, 1869

13. **Tang, C.W. and S.A. van Slyke**, Organic Electroluminescent Diodes. **Applied Physics Letters**, 1987. **51**(12): p. 913-915.

14. **Tatemichi, S., et al.**, High mobility n-type thin-film transistors based on N,N'-ditridecyl perylene diimide with thermal treatments. **Applied Physics Letters**, 2006. **89**(11).

15. **Jones, B.A., et al.**, Tuning orbital energetics in arylene diimide semiconductors. Materials design for ambient stability of n-type charge transport. **Journal of the American Chemical Society**, 2007. **129**(49): p. 15259-15278.

16. **Allwood, D.A., et al.**, Magneto-optical Kerr effect analysis of magnetic nanostructures. **Journal of Physics D-Applied Physics**, 2003, **36**(18): p. 2175-2182.

17. **Fischer, P.**, Viewing spin structures with soft X-ray microscopy, **Materials Today**, 2010, **13**(9) 14

18. **Bryan, M.T., et al.**, Observation of field-induced domain wall propagation in magnetic nanowires by magnetic transmission X-ray microscopy, **J. Appl. Phys.**, 2008, **103**, 07D909

19. **Kirk, K.J.**, Nanomagnets for sensors and data storage. **Contemporary Physics**, 2000. **41**(2): p. 61-78.

20. **Basu, S., et al.**, Control of the switching behavior of ferromagnetic nanowires using magnetostatic interactions. **Journal of Applied Physics**, 2009. **105**(8).

21. **Cowburn, R.P., et al.**, Domain wall injection and propagation in planar Permalloy nanowires. **Journal of Applied Physics**, 2002. **91**(10): p. 6949-6951.

22. **O'Handley, R.C.**, Modern magnetic materials : principles and applications. 2000, New York ; Chichester: Wiley.

23. **Cowburn, R.P. et al.**, Magnetic domain wall propagation in nanowires under transverse magnetic fields. **J. Appl. Phys.**, 2002, **91**, 6949.

24. **Schrefl, T., et al.**, Domain structures and switching mechanisms in patterned magnetic elements. **J. Magn. Magn. Mater.**, 1997, **175**, 193.

25. **O'Brien, L., et al.**, Magnetic domain wall induced, localized nanowire reversal. **Phys. Rev. Lett.** 2011, **106**, 087204.

26. **Hayward, T.J., et al.**, Pinning induced by inter-domain wall interactions in planar magnetic nanowires. **Appl. Phys. Lett.** 2010, **96**, 052502.

27. **Hayward, T.J., et al.**, Direct imaging of domain-wall interactions in Ni₈₀Fe₂₀ planar nanowires. **PHYSICAL REVIEW B** 2010, **81**, 020410.

28. **Dediu, V. et al.**, Room-temperature spintronic effects in Alq₃-based hybrid devices. **Physical Review B**, 2008, **78**, 115203.